Inorg. Chem. **2000,** *39,* 3320−3324

Synthesis and Characterization of the Layered Vanadium Borophosphate $(\mathrm{Imidazolium})_{3.8}(\mathrm{H_3O})_{1.2}[(\mathrm{VO})_4(\mathrm{BO})_2(\mathrm{PO_4})_5]\cdot 0.3\mathrm{H_2O}$

Ranko P. Bontchev, Junghwan Do, and Allan J. Jacobson*

Department of Chemistry, University of Houston, Houston, Texas 77204-5641

Received February 18, 2000

The first layered vanadium borophosphate $(\mathrm{imidazolium})_{3.8}(\mathrm{H_3O})_{1.2}[(\mathrm{VO})_4(\mathrm{BO})_2(\mathrm{PO_4})_5]\cdot 0.3\mathrm{H_2O}$ (**1**) has been synthesized hydrothermally and characterized by chemical analysis, infrared and Raman spectroscopy, and thermogravimetric and magnetic measurements. The compound crystallizes in the monoclinic space group $C2/c$, $a = 9.4737$ (5) Å, $b = 22.1444$ (12) Å, $c = 17.2192$ (13) Å, $\beta = 105.936$ (1)°, $Z = 4$. The structure contains a novel borophosphate secondary building unit, $[\mathrm{B_2P_5O_{22}}]$, in which two $\mathrm{BP_2O_{10}}$ trimers are linked by an additional $\mathrm{PO_4}$ tetrahedron. These units are connected by $\mathrm{V(IV)_2O_8}$ dimers and $\mathrm{V(IV)O_5}$ square pyramids to form layers. The space between the layers is filled by disordered imidazolium and hydronium cations and water molecules that form a complex network of hydrogen bonds. A model for the interlayer disorder is proposed.

Introduction

Several new synthetic metal borophosphates (MBPOs) recently have been synthesized and structurally characterized.[1] A large variety of new structural types are observed among these compounds, including cluster anions[2−5] and one-, two-, and three-dimensional arrangements of MBPO units.[1]

The anionic borophosphate $(\mathrm{B}_x\mathrm{P}_y\mathrm{O}_z)^{n-}$ components of these structures are of particular interest. Depending on the B:P ratio, different secondary BPO building units are formed.[1] As in other complex oxide structures, the type and arrangement of the BPO units in a particular structure depend on the charge, size, and nature of the inorganic and/or organic countercations. The following examples illustrate some of the variety. One of the most common BPO units, found in almost half of the synthetic MBPOs, is the $\mathrm{BP_2O_{10}}$ trimer. This trimer contains a $\mathrm{BO_4}$ tetrahedron which shares two of its oxygen atoms with two $\mathrm{PO_4}$ tetrahedra. Combinations of $\mathrm{BP_2O_{10}}$ trimers with different M countercations result in totally different structural arrangements. For example, isolated $\mathrm{BP_2O_{10}}$ trimers are present in $\mathrm{NaFe[BP_2O_7(OH)_3]}$, whereas in $\mathrm{K_2Fe_2[B_2P_4O_{16}(OH)_2]}$, two $\mathrm{BP_2O_{10}}$ trimers are linked together to form four-membered $(\mathrm{BO_{3/2}O_{1/1}}\text{-}\mathrm{PO_{2/2}O_{2/1}})_2$ rings.[6] In the structure of $\mathrm{Na_4Cu_3[B_2P_4O_{15}(OH)_2]}\cdot 2\mathrm{HPO_4}$ two $\mathrm{BP_2O_{10}}$ trimers form the same four-membered ring but with an additional $\mathrm{BO_3{-}O{-}BO_3}$ bond.[7] Similar units are found in the chain structure of $\mathrm{Na_5[B_2P_3O_{13}]}$.[8] More complex arrangements are found in the structures of $\mathrm{Na_{1.89}Ag_{0.11}[BP_2O_7(OH)]}$, $\mathrm{Na_2[BP_2O_7(OH)]}$,[9] and $\mathrm{K_6Cu_2[B_4P_8O_{28}(OH)_6]}$[7] and in the infinite chain structure of $\mathrm{CsFe[BP_2O_8(OH)]}$.[10] In $\mathrm{M^IM^{II}(H_2O)_2[BP_2O_8]\cdot H_2O}$ ($\mathrm{M^I}$ = Na, K; $\mathrm{M^{II}}$ = Mg, Mn, Fe, Co, Ni, Zn) the $\mathrm{BP_2O_{10}}$ trimers are linked together in infinite one-dimensional double helices.[11]

We are investigating the vanadium borophosphates (VBPOs)[2−5,12,13] as part of a systematic study of MBPOs. The structures of all but two of the recently synthesized VBPOs contain the $\mathrm{BP_2O_{10}}$ building units discussed above. Several examples contain $\mathrm{BP_2O_{10}}$ trimers which alternate with $\mathrm{V_2O_8}$ dimers, and different structures are observed with different countercations. In a recent paper, we have shown that the $\mathrm{V_2O_8}$ and $\mathrm{BP_2O_{10}}$ units can be assembled into cluster anions of different sizes in a controlled way by varying the specific cation used in the reaction.[4] For example, in $\mathrm{(C_4H_{12}N_2)_6[(VO)_2BP_2O_{10}]_4}\cdot n\mathrm{H_2O}$ (pip−VBPO), four $\mathrm{V_2O_8}$ and four $\mathrm{BP_2O_{10}}$ units form a four-membered cyclic anion, while in $\mathrm{Na_{14}\{Na{\supset}[(VO)_2BP_2O_{10}]_5\}}\cdot n\mathrm{H_2O}$ (Na−VBPO) the resulting structure contains a five-membered cyclic anion.[4,2] In the same way, the $\mathrm{V_2O_8}$ and $\mathrm{BP_2O_{10}}$ units are arranged in six-membered cyclic anions in $\mathrm{A_{17}\{A{\supset}[(VO)_2BP_2O_{10}]_6\}}\cdot n\mathrm{H_2O}$ (A = $\mathrm{NH_4^+}$, $\mathrm{K^+}$, $\mathrm{Rb^+}$, $\mathrm{Cs^+}$) (A−VBPOs) and $\mathrm{NH_4(C_3H_{12}N_3)_8\{[NH_4{\supset}[V_2P_2BO_{12}]_6\}}\cdot 15\mathrm{H_2O}$.[5] In contrast, $\mathrm{(C_2H_{10}N_2)_2\ [(VO)_5(H_2O)BP_2O_{10}]}\cdot 1.5\mathrm{H_2O}$ contains one-dimensional chains of alternating $\mathrm{V_2O_8}$ and $\mathrm{BP_2O_{10}}$ units joined together by $\mathrm{VO_6}$ octahedra to form a three-dimensional structure.[12]

In the present work, we report the first example of a layered vanadium borophosphate, $(\mathrm{imidazolium})_{3.8}(\mathrm{H_3O})_{1.2}[(\mathrm{VO})_4(\mathrm{BO})_2(\mathrm{PO_4})_5]\cdot 0.3\mathrm{H_2O}$ (**1**). In the structure of **1**, two $\mathrm{BP_2O_{10}}$ trimers are linked together by an additional $\mathrm{PO_4}$ tetrahedron to form a new $\mathrm{B_2P_5O_{22}}$ building unit.

---

* To whom correspondence should be addressed. Phone: (713) 743-2785. Fax: (713) 743-2787. E-mail: ajjacob@uh.edu.

(1) Kniep, R.; Engelhardt, H.; Hauf, C. *Chem. Mater.* **1998**, *10*, 2930−2934.
(2) Warren, C. J.; Haushalter, R. C.; Rose, D. J.; Zubieta, J. *Inorg. Chem. Commun.* **1998**, *1*, 4−6.
(3) Bontchev, R. P.; Do, J.; Jacobson, A. J. *Inorg. Chem.* **1999**, *38*, 2231−2233.
(4) Bontchev, R. P.; Do, J.; Jacobson, A. J. *Angew. Chem., Int. Ed. Engl.* **1999**, *38*, 1937−1940.
(5) Do, J.; Zheng, L.-M.; Bontchev, R. P.; Jacobson, A. J. *Solid State Sci.* **2000**, *3*, 343−352.
(6) Boy, I.; Cordier, G.; Eisenmann, B.; Kniep, R. *Z. Naturforsch., B: Chem. Sci.* **1998**, *53*, 165−170.
(7) Boy, I.; Cordier, G.; Kniep, R. *Z. Kristallogr.−New Cryst. Struct.* **1998**, *213*, 29−30.
(8) Hauf, C.; Friedrich, T.; Kniep, R. *Z. Kristallogr.* **1995**, *210*, 446.
(9) Kniep, R.; Engelhardt, H. *Z. Anorg. Allg. Chem.* **1998**, *624*, 1291−1297.
(10) Engelhardt, H.; Kniep, R. *Z. Kristallogr.−New Cryst. Struct.* **1999**, *214*, 443−444.
(11) Kniep, R.; Will, H. G.; Boy, I.; Rohr, C. *Angew. Chem., Int. Ed. Engl.* **1997**, *36*, 1013−1014.
(12) Warren, C. J.; Haushalter, R. C.; Rose, D. J.; Zubieta, J. *Chem. Mater.* **1997**, *9*, 2694−2696.
(13) Zhao, Y.; Zhu, G.; Liu, W.; Zou, Y.; Pang, W. *J. Chem. Soc., Chem. Commun.* **1999**, 229−230.

10.1021/ic000177u CCC: $19.00

Experimental Section

Synthesis. 1 was synthesized by reaction of V_2O_3 (0.2248 g, 1.5 mmol), H_3BO_3 (0.3090 g, 5 mmol), H_3PO_4 (0.342 mL, 5 mmol, 85 wt % solution in H_2O), $CuCl_2$ (0.150 g, 1 mmol), $N_2C_3H_4$ (0.300 g, 5 mmol), and 2 mL of H_2O. The reaction was carried out in a 23 mL capacity Teflon-lined stainless steel Parr hydrothermal bomb and heated at 160 °C for 3 d. The pH value after the reaction completion was 2.74. Transparent deep blue crystals of **1**, average size 0.1−0.3 mm, yield 60% based on vanadium, were formed in the reaction product. A second green polycrystalline phase was also formed. An infrared spectrum suggested that this compound was a vanadium phosphate, but it was not characterized further.

1 could be synthesized only in the presence of Cu^{2+}. We were unable to synthesize the title compound by varying the reaction conditions in the absence of Cu^{2+}. The only other known vanadium borophosphate with an extended structure, $[H_3NCH_2CH_2NH_3]_2[(VO)_5(H_2O)\{O_3POB(O)_2OPO_3\}_2]\cdot 1.5H_2O$, was also synthesized in the presence of Cu^{2+}.[12] The reason for the influence of $CuCl_2$ on the crystallization behavior of these phases is unknown.

X-ray Crystallography. A blue polyhedral crystal of approximate dimensions 0.20 × 0.15 × 0.10 mm was mounted on a SIEMENS SMART X-ray diffractometer with a 1 K CCD area detector. Data were collected using graphite-monochromatized Mo Kα radiation (λ = 0.710 73 Å) at room temperature. A hemisphere of data (1271 frames at a 5 cm detector distance) was collected using a narrow-frame method with scan widths of 0.30° in ω and an exposure time of 30 s/frame. The first 50 frames were remeasured at the end of the data collection to monitor instrument and crystal stability, and the maximum correction applied on the intensities was <1%. The data were integrated using the Siemens SAINT program[14] with intensity corrections for the Lorentz factor, polarization, air absorption, and absorption due to variations in the path length through the detector faceplate. A total of 4019 independent reflections were collected within the range $1.84° < \theta < 28.56°$. A ψ scan was used for the absorption correction.

The structure was solved by direct methods followed by full-matrix least-squares refinement with the SHELXTL software package.[15] Vanadium, phosphorus, oxygen, and boron atoms were first located and their thermal parameters refined anisotropically. The disordered imidazolium cations were then located and their positions and occupancies refined using a rigid body model. Equivalent C−C and C−N distances of 1.37 Å based on the crystal structure of imidazole were used.[16] The assignment of the nitrogen and carbon atoms was made by considering the possible N−H···O hydrogen bonds. The occupancies were refined until the values of the isotropic thermal parameters became on the order of 0.048−0.051. Only the thermal parameters of one disordered imidazolium cation were refined anisotropically since the occupancy factors of the others were less than 0.5. Finally positions for the disordered water molecules were located and their occupancies refined until the values of the isotropic thermal parameters became on the order of 0.05−0.06. The final cycle of refinement performed on F_o^2 resulted in $R = 0.049$ and $R_w = 0.108$. The crystallographic data are listed in Table 1.

Characterization. Elemental analysis (Galbraith Laboratories, Inc.) confirmed the V:P:B = 4:5:2 ratio determined by the crystal structure refinement, found V:P:B = 4:4.84:2.22. Infrared spectra were recorded on a Matteson FTIR 5000 spectrometer within the range 400−4000 cm^{-1}, by using the KBr pellet method. Raman spectra were measured using the He−Ne laser line (632.8 nm) and a CCD spectrometer, laser spot 5−7 μm, 0.6 mW, average laser power density 1000−2000 $W\cdot cm^{-2}$. Thermogravimetric analysis was carried out in air at a heating rate of 1 °C/min (high-resolution TGA 2950 thermogravimetric analyzer). Magnetic data were obtained in the temperature range 4 K < T < 290 K with an applied magnetic field of 0.1 T by using a Quantum Design MPMS SQUID XL magnetometer.

Table 1. Crystallographic Data for **1** $[(\text{imidazolium})_{3.8}(H_3O)_{1.2}[(VO)_4(BO)_2(PO_4)_5]\cdot 0.3H_2O]$

empirical formula	$C_{5.70}H_{9.50}BN_{3.80}O_{13.75}P_{2.50}V_2$	Z	4
		space group	$C2/c$ (no. 15)
fw	1086.93	T, K	293
cryst size, mm^3	0.2 × 0.15 × 0.1	λ, Å	0.710 73
a, Å	9.4737(5)	ρ_{calcd}, g cm^{-3}	2.070
b, Å	22.1444(12)	μ, mm^{-1}	1.387
c, Å	17.2192(13)	R,[a] R_w[b] [$I > 2\sigma(I)$]	0.0493, 0.1079
β, deg	105.936 (1)		
V, $Å^3$	3473.6(4)		

[a] $R = \sum||F_o| - |F_c|/\sum|F_o|$. [b] $R_w = [\sum w(|F_o| - |F_c|)^2/\sum w|F_o|2]^{1/2}$; $w = 1/[\sigma^2(F_o^2) + (0.0339P)^2 + 28.04P]$; $P = [\max(F_o^2,0) + 2F_c^2]/3$.

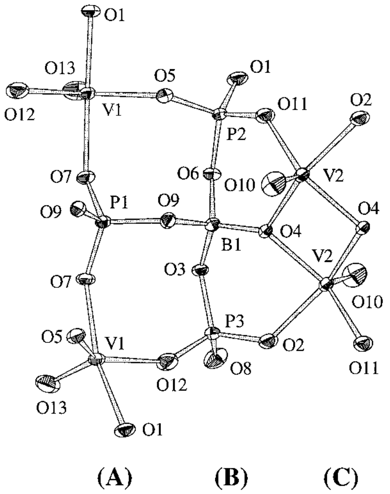

Figure 1. Inorganic building unit in **1**, 50% thermal ellipsoids. Note the three distinct secondary building units, A, B, and C (see the text).

Results

Crystal Structure. (1) Layer Structure. The vanadium atoms occupy two crystallographically independent general positions. Each vanadium is coordinated by five oxygen atoms to form a square pyramid with one short V═O apical vanadyl bond (V1═O13 = 1.587 Å, V2═O10 = 1.592 Å) and four basal V−O bonds of average length ∼2.0 Å (V1−O = 1.979 Å, V2−O = 1.970 Å), Figure 1, Table 2. Bond valence sum (BVS) calculations,[17] as well as magnetic measurements (see below), confirmed that all vanadium atoms are V^{4+} (BVS 4.11 and 4.09 found for V1 and V2, respectively).

All of the basal oxygen atoms of the $V1O_5$ pyramids (O1, O5, O7, O12) are shared with PO_4 tetrahedra. The V_2O_5 pyramids (O2, O4, O10, O11) are linked by sharing a common edge (O4−O4) to form $[V_2O_8]$ dimers. Two of the basal oxygen atoms (O2 and O11) are shared with PO_4 tetrahedra and two O4 atoms with BO_4 tetrahedra (Figure 1).

The phosphorus atoms occupy three independent positions and are coordinated by four oxygen atoms in almost regular tetrahedra. Two of the oxygen atoms (O7) coordinated to P1 are shared with vanadium atoms (V1), and two are shared with boron atoms (O9). Three of the oxygen atoms (O1, O5, O11) coordinated to P2 are shared with vanadium atoms (V1, V2), and one (O6) is shared with a boron atom. Two of the oxygen atoms (O2, O12) coordinated to P3 are shared with vanadium atoms (V1, V2), one (O3) is shared with a boron atom, and the remaining oxygen (O8) is terminal. The boron atoms are coordinated by four oxygen atoms to form a nearly regular tetrahedron. Three of these oxygen atoms (O3, O6, O9) are

---

(14) SAINT Version 4.05, Siemens Analytical X-ray Instruments, Madison, WI, 1995.

(15) Sheldrick, G. M. SHELXTL Version 5.03, Siemens Analytical X-ray Instruments, Madison, WI, 1995.

(16) Craven, B. M.; McMullan, R. K.; Bell, J. D.; Freeman, H. C. *Acta Crystallogr.* **1977**, *B33*, 2585.

(17) Brese, N. E.; O'Keeffe, M. *Acta Crystallogr.* **1991**, *B47*, 192.

Table 2. Selected Bond Lengths (Å) for **1**[a]

V1−O13	1.587(2)	V2−O10	1.592(2)
V1−O12	1.926(2)	V2−O4	1.963(2)
V1−O5	1.928(2)	V2−O11	1.963(2)
V1−O7	2.029(2)	V2−O2	1.977(2)
V1−O1	2.033(2)	V2−O4	1.977(2)
P1−O7	1.513(2)	P2−O5	1.519(2)
P1−O7	1.513(2)	P2−O11	1.528(2)
P1−O9	1.561(2)	P2−O1	1.524(2)
P1−O9	1.561(2)	P2−O6	1.568(2)
P3−O12	1.508(2)	B1−O4	1.438(2)
P3−O2	1.525(2)	B1−O3	1.465(2)
P3−O8	1.529(2)	B1−O6	1.485(2)
P3−O3	1.554(2)	B1−O9	1.514(2)
O1···H13	1.984(4)	O10···H54	2.174(5)
O1···H21	2.086(4)	O_{W70}···H52	2.109(4)
O2···H51	2.016(5)	O_{W41}···O7	2.974(5)
O6···H11	2.015(4)	O_{W41}···O8	2.804(5)
O6···H34	2.162(4)	O_{W42}···O8	2.820(5)
O4···H75	2.091(5)	O_{W71}···O5	2.943(5)
O7···H41	1.999(4)	O_{W71}···O9	3.128(5)
O9···H53	2.119(4)		

[a] Symmetry transformations used to generate equivalent atoms: (1) $-x-1, -y, -z$, (2) $-x+1, y, -z+1/2$, (3) $-x, y, -z+1/225$, (4) $-x, -y, -z$.

shared with phosphorus (P1, P2, P3), and one (O4) is shared with two V2 vanadium atoms.

The inorganic part of the structure can be described as built up from three different units. The first unit consists of one PO_4 tetrahedron and two vanadium square pyramids with the composition $[V_2PO_{12}]$ (Figure 1). The second unit consists of two PO_4 tetrahedra and one borate tetrahedron connected by sharing corners to form $[BP_2O_{10}]$ trimers. The third unit is the $[V_2O_8]$ dimer, which is connected to two $[BP_2O_{10}]$ trimers. If we denote the $[V_2PO_{12}]$, $[BP_2O_{10}]$, and $[V_2O_8]$ units as A, B, and C, respectively, one-dimensional chains along *c*, with the sequence [···ABCBABCBA···] (Figure 2a) are linked together by the O1 oxygen atoms to form undulating layers (Figure 2b). The connectivity among the VO_5, PO_4, and BO_4 polyhedra results in the layer composition $[V_4B_2P_5O_{26}]$.

(2) Interlayer Structure. The interlayer space is filled by disordered protonated imidazole and hydronium cations and water molecules that link the layers through a complex network of hydrogen bonds (Figures 2b and 3). The disorder is complex but has been modeled by using the rigid body description of the imidazolium cations and by considering the constraints on the site occupancies. A consistent, though not necessarily unique, model for the interlayer structure has been obtained. For simplicity, in the following discussion hydronium cations and water molecules will be described as water molecules since they cannot be distinguished in the X-ray refinement.

The disordered imidazolium cations form three distinct sets, denoted I_{123}, I_4, and I_{567} (see Figure 2b). The I_{123} and I_{567} sets each contain three separate imidazolium cations in general positions, and therefore, the total number of imidazolium cations in each of these sets must be ≤1. The shortest distances between any hydrogen atoms of the imidazolium cations of the I_{123} and I_{567} groups are equal to or larger than 2.38 Å, and therefore, these sets can be simultaneously and fully occupied. The third type of imidazole, I_4, contains only one molecule occupying a general position. The closest distances between some of the equivalent hydrogen atoms generated by the 2-fold axis are on the order of only 1.05 Å. Consequently, this site cannot be fully occupied, and the occupancy factor must be ≤0.5. Similar steric restrictions arise if we consider the separation between the I_4 and I_{567} sets of imidazolium cations. The closest distances between some of the hydrogen atoms of I_4 and some symmetry equivalents of I_{567} are only about 0.5 Å. The total occupancy of I_4 and I_{567} is constrained by these interactions to be ≤1.

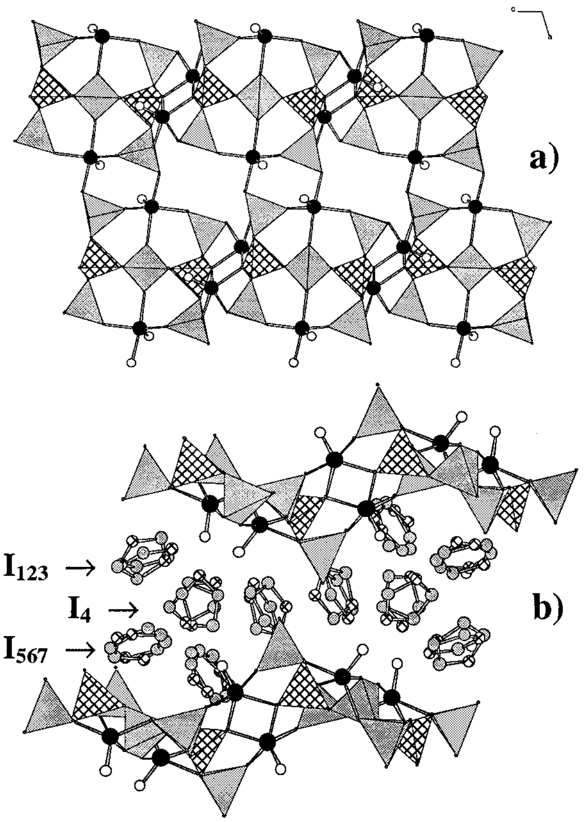

Figure 2. Structure of **1**: (a) view of the VBPO layers along *b* and (b) view of the structure along *c*. PO_4 and BO_4 are shown as gray and hatched tetrahedra and vanadium, oxygen, carbon, and nitrogen atoms as black, open, gray, and hatched circles, respectively. The disordered water molecules are omitted for clarity. The three sets of disordered imidazolium cations are labeled I_{123}, I_4, and I_{567}, respectively.

The interlayer structure is complicated by disordered water molecules located in positions similar to those of the imidazolium cations. Two different water molecules, W70 and W71, occupy positions similar to those of the I_{567} set. The oxygen atoms of these water molecules occupy two independent general positions and are separated by 2.74 Å. Both sites can, therefore, be fully and simultaneously occupied. If we take into account the occupancy restrictions for the I_{567} set, then total occupancy factors for I_{567} + W70 + W71 must be ≤1. Water molecules are also located in three positions (W41, W42, and W43) near the I_4 imidazole site. Analysis of the occupancies and intermolecular distances revealed that each imidazole can be substituted by one water molecule. Taking into account the occupancy restrictions for I_4, the total occupancy of W41 + W42 + W43 must be ≤0.5.

Two examples illustrate the effect of these occupancy constraints on the composition of the interlayer. If the I_{123} and I_4 sets are fully occupied, then the I_{567} set contains no imidazolium cations, but two water molecules are in similar positions. Hence, the first limiting composition is $(imidazolium)_4(H_3O)[V_4B_2P_5O_{26}]$. In the other limiting case, the I_{123} and I_{567} sets are fully occupied, and two water molecules are located near the I_4 position. This limiting composition is $(imidazolium)_3(H_3O)_2[V_4B_2P_5O_{26}]\cdot 2H_2O$. Any of the compositions between these limits is allowed, and it is possible that a large number of different compositions occur within the same reaction batch (see below). The final refinement of the crystal structure resulted in

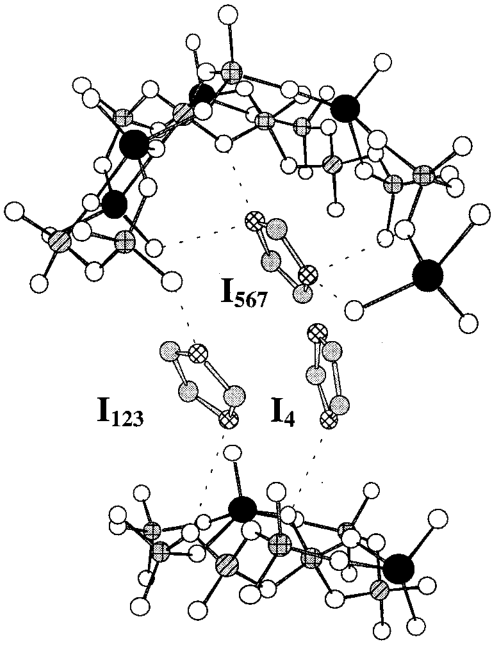

Figure 3. Hydrogen bonding (dotted lines) in **1**. Only one of the three disordered imidazolium molecules in sets I_{123} and I_{567} is shown for clarity. Vanadium, phosphorus, boron, oxygen, nitrogen, and carbon atoms are shown as black, gray cross-hatched, gray hatched, open, white cross-hatched, and gray circles, respectively.

the composition $(\text{imidazolium})_{3.8}(H_3O)_{1.2}[V_4B_2P_5O_{26}]\cdot 0.3H_2O$ within the above limits. The fact that the imidazole content is close to the upper limit and the excellent quality of the measured crystal suggest a correlation.

The reasons for the disorder can be understood by analysis of the hydrogen bonds between the imidazole and water molecules and the oxygen atoms from the VBPO layers. All three imidazolium cations of the I_{123} set form N−H···O bonds as shown in Figure 3. The three different sets of nitrogen atoms, however, are linked to different oxygen atoms by hydrogen bonds of almost equal distances (Table 2). Hence, there is no particular reason why any of the three possible orientations of the imidazolium cations should be preferred. The same argument applies to the imidazolium cations of the I_4 and I_{567} sets.

The directions of the N−H···O bonds and hence the role of each of the imidazolium cations, however, are quite different, Figures 2b and 3. Each imidazolium cation of the I_{123} set is bonded to oxygen atoms of two adjacent VBPO layers. This together with the full occupancy of the I_{123} set suggests that these hydrogen bonds determine the interlayer bonding and the overall structure. Hydrogen bonds exist between the VBPO layers and the I_4 imidazolium cations, but the low site occupancy suggests that they are less significant. The imidazolium cations in the I_{567} sets form hydrogen bonds with only one VBPO layer, indicating a simple space-filling role.

Characterization. Thermogravimetric studies revealed that upon heating in air **1** loses the interlayer H-imidazole and H_2O below 600 °C. An initial weight loss of 2.66% corresponds to the loss of interlayer water. A second weight loss (22.25%) between 225 and 425 °C corresponds to the loss of the imidazolium cations. The final step (2.0%) due to dehydroxylation occurs above 450 °C. At 600 °C, the product is a glassy residue. Assuming a final composition of $4VO_2\cdot 2.5P_2O_5\cdot B_2O_3$, then the weight loss calculated for the second two steps assuming three imidazoles per formula unit is 24.78% compared with the measured value of 24.45%. The water content is found to be $1.62H_2O$ from the initial weight loss. The weight loss begins immediately after the sample is loaded onto the thermogravimetric analyzer at ambient temperature, and therefore 1.62 represents a lower limit. The composition from the TGA measurements differs somewhat from that obtained from the refined X-ray structure but is within the limits proposed above.

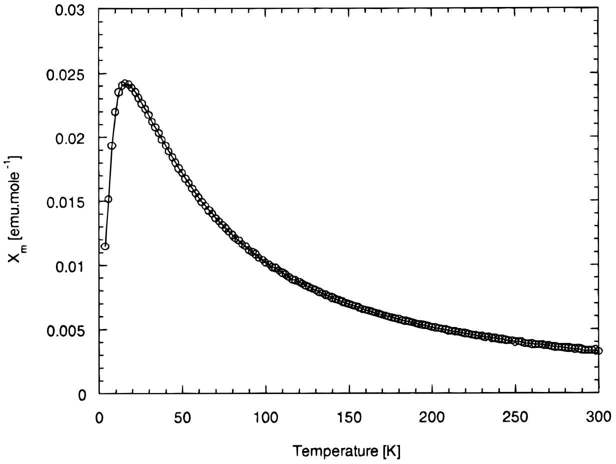

Figure 4. Molar magnetic susceptibility of **1** as a function of temperature.

The strongest bands in the infrared and Raman spectra of **1** are similar to those observed in other vanadium borophosphates[3−5] and are summarized below. A detailed vibrational (IR and Raman) study on a series of vanadium borophosphates is in progress.

Infrared: 418 (w), 468 (m), 490 (w), 554 (w), 583 (m), 626 (m), 688 (m), 770 (sh), 817 (s), 903 (sh), 960 (m), 978 (m), 1018 (s), 1054 (s), 1090 (s), 1160 (m), 1445 (m), 1592 (m), and 1628 (m) cm^{-1}. Raman: 406 (w), 432 (w), 468 (w), 530 (m), 578 (m), 625 (w), 671 (w), 765 (w), 909 (w), 961 (sh), 995 (s), 1015 (vs), 1055 (w), 1104 (w), 1132 (w), 1210 (s), 1455 (s), and 1591 (w) cm^{-1}.

Magnetic measurements of **1** showed a complex behavior, Figure 4. At high temperatures (50−300 K) the sample is paramagnetic and obeys the Curie−Weiss law. The data were modeled in the temperature range 50 K $\leq T \leq$ 250 K with the equation $\chi_M = \chi_0 + C/(T - \Theta)$, giving values of $\chi_0 = -0.000\,37(1)$ emu/mol, $C = 0.376(3)$ emu K/mol, and $\Theta = -32.3(5)$ K. Assuming $g = 2.0$, the observed magnetic moment of 1.73 μ_B per vanadium ion is consistent with a formula containing only V^{4+} ions. Below 50 K, the magnetic suceptibility goes through a broad maximum indicative of antiferromagnetic exchange coupling between the V_2O_8 dimers and the isolated VO_5 square pyramid.

Discussion

The structure of **1** can be compared to the structures of several other vanadium borophosphates. In the compounds pip−VBPO,[4] Na−VBPO,[4] en−VBPO,[12] and NH_4−VBPO,[4] $[BP_2O_{10}]$ (B) and $[V_2O_8]$ (C) units are arranged in cyclic cluster anions of composition $[BC]_4$, $[BC]_5$, and $[BC]_6$, respectively. In en−VBPO, one-dimensional chains of composition $[BC]_\infty$ are linked together by VO_6 octahedra to form an extended three-dimensional structure. In this context, the structure of **1** can be considered as an intermediate case where [BCB] building blocks are linked by $[V_2PO_{12}]$ (A) units to form a two-dimensional structure.

If we consider only the BPO anionic part of the structure, a new building unit, $[B_2P_5O_{22}]$, can be defined (Figure 2a). This unit is closely related to the units discussed above. In **1** two

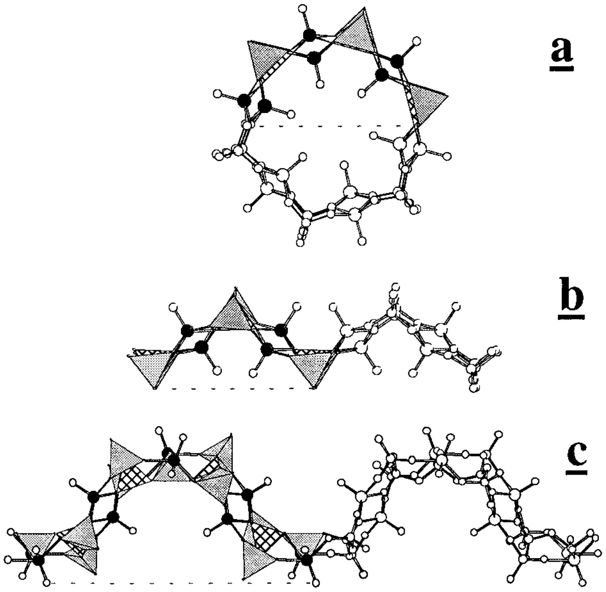

Figure 5. Orientations of the terminal phosphate oxygen atoms in (a) cyclic A−VBPO (A = NH_4, K, Rb, Cs) clusters,[4] (b) en−VBPO,[12] and (c) imid−VBPO (present work). PO_4 and BO_4 are shown as gray and hatched tetrahedra and vanadium and oxygen atoms as black and open circles, respectively.

$[BP_2O_{10}]$ units are linked together by an additional PO_4 tetrahedron connected to the two BO_4 tetrahedra, Figure 1. This unit has no P−O−P bonding as expected for secondary BPO building units.[1]

The B:P ratio affects the nature of the BPO units. In all the structures with a B:P ratio of 1:2, $[BP_2O_{10}]$ trimers can be observed as distinct building units linked together in different ways.[1,2,4,6,9,11,12,18] When the B:P ratio is decreased to 1:3, however, the resulting BPO units are branched chains as in $M_3[BP_3O_{12}]$ (M = Ba, Pb),[19,20] condensed units with nominal composition B:P = 1:2 plus separate PO_4 groups as in $Na_4Cu_3[B_2P_4O_{15}(OH)_2]\cdot 2HPO_4$,[7] or BO_3−PO_4 dimers plus separate PO_4 groups as in $Co_5[BP_3O_{14}]$.[21] The composition of **1** has an intermediate B:P ratio of 1:2.5, and the $[BP_2O_{10}]$ trimers still exist as distinct units. A B:P = 1:2.5 ratio may be the lower limit below which condensation and/or branching of the $[BP_2O_{10}]$ units together with segregation of the "additional" PO_4 groups takes place.

It is interesting to compare the relative orientations of the terminal oxygen atoms of the PO_4 groups in the $[BP_2O_{10}]$ units on either side of the V_2O_8 dimers in different compounds. In all of the VBPOs discussed above, as well as in **1**, each $[V_2O_8]$ dimer is sandwiched between two $[BP_2O_{10}]$ units (BCB). In all four-, five-, and six-membered cyclic VBPO cluster anions the terminal phosphate oxygen atoms are in a cis configuration relative to the basal plane of the V_2O_8 dimers (Figure 5a). In extended structures such as en−VBPO and **1**, the orientation of these oxygen atoms is trans with respect to the VBPO planes (Figure 5b,c).

In the case of the cyclic anions, the principal structure directing force appears to be the presence of cations of proper size and charge around which the $[V_2O_8]$ and $[BP_2O_{10}]$ units assemble and link in a way that provides the optimum cation coordination. As a result, under similar reaction conditions the five-membered cluster is formed with Na^+ in the center of the anion, whereas the larger cations, NH_4^+, K^+, Rb^+, Cs^+, direct the synthesis to the six-membered anion.[4]

In the extended structures the V_2O_8 and $[BP_2O_{10}]$ units are arranged in chains that "bend" around larger organic cations, and significant hydrogen-bonding interactions are present between the organic cations and the oxide framework. For example, in en−VBPO the magnitude of the chain bending (or the "wavelength" and the "amplitude" of the VBPO chains) is determined both by the size of the ethylenediammonium cations and by the directions of the NH···O hydrogen bonds. In this particular case, the optimum is achieved by an arrangement in which the terminal phosphate oxygen atoms of the $[BP_2O_{10}]$ units are trans to the basal plane of the vanadium dimers. The wavelength and the amplitude of the VBPO chains in the structure of **1** are determined in a similar way by the interlayer imidazolium cations. The specific requirements of the cation packing and hydrogen bonding result in the introduction of an additional building unit and a longer wavelength and amplitude for the chain.

The piperazine−VPBO structure contains a four-membered cluster anion rather than a chain and is an interesting anomaly. In this case, the anion does not contain a central cation and the countercation, protonated piperazine, forms a network of intercluster hydrogen bonds. The conditions used in the synthesis of the cyclic clusters and the extended structures, however, differ in respects other than the use of specific cations. We are, at present, making a systematic investigation of reaction conditions that direct the formation of cis or trans building units in an attempt to control the synthesis of new VPBO structures.

Conclusions

In conclusion, the first example of layered vanadium borophosphate, $(imidazolium)_{3.8}(H_3O)_{1.2}[(VO)_4(BO)_2(PO_4)_5]\cdot 0.3H_2O$, has been synthesized and characterized by chemical analysis, single-crystal X-ray diffraction, infrared and Raman spectroscopy, and thermogravimetric and magnetic measurements. The structure contains a novel secondary building BPO unit, $[B_2P_5O_{22}]$. The relative orientation (trans and cis) of the $[BP_2O_{10}]$ trimers in the title compound and in the cyclic clusters and chains of composition $[V_2BP_2O_{12}]_n$ (n = 4, 5, 6, ∝) suggest possible new phases formed by combinations of cis and trans arrangements of building units.

Acknowledgment. This work was supported by the National Science Foundation under Grant DMR-9805881 and by the Robert A. Welch Foundation. The work made use of MRSEC/TCSUH Shared Experimental Facilities supported by the National Science Foundation under Award Number DMR-9632667 and the Texas Center for Superconductivity at the University of Houston. We also thank Milko Iliev for the Raman spectra and Marcos Dezanetti for the magnetic data.

Supporting Information Available: An X-ray crystallographic file in CIF format for the structure determination of $(imidazolium)_{3.8}(H_3O)_{1.2}[(VO)_4(BO)_2(PO_4)_5]\cdot 0.3H_2O$ (**1**). This material is available free of charge via the Internet at http://pubs.acs.org.

IC000177U

---

[18] Hauf, C.; Kniep, R. *Z. Naturforsch., B: Chem. Sci.* **1997**, *52*, 1432−1435.

[19] Kniep, R.; Goezel, G.; Eisenmann, B.; Roehr. *Angew. Chem.* **1994**, *106*, 791−3; *Angew. Chem., Int. Ed. Engl.* **1994**, *33* (7), 749−51.

[20] Park, C. H.; Bluhm, K. *Z. Naturforsch.* **1995**, *50b*, 1617−1622.

[21] Bontchev, R. P.; Sevov, S. C. *Inorg. Chem.* **1996**, *35*, 6910−6911.